

# Large-scale correlated study of excited state absorptions in naphthalene and anthracene

Priya Sony and Alok Shukla

*Department of Physics, Indian Institute of  
Technology Bombay, Powai, Mumbai 400076, INDIA.*

## Abstract

In this paper, we report theoretical calculations of the photo-induced absorption (PA) spectrum of naphthalene and anthracene, with the aim of understanding those excited states, which are invisible in the linear optical absorption. The excited state absorption spectra are computed from the  $1B_{2u}^+$  and the  $1B_{3u}^+$  states, and a detailed analysis of the many-body character of the states contributing to various peaks in the spectra is presented. The calculations are performed using the Pariser-Parr-Pople (PPP) Hamiltonian, along with the full configuration interaction (FCI) technique. The role of Coulomb parameters used in the PPP Hamiltonian is examined by considering standard Ohno parameters, as well as a screened set of parameters. The results of our calculations are extensively compared with the experimental data where available, and very good agreement has been obtained. Moreover, our calculations predict the presence of high intensity features which, to the best of our knowledge have not been explored earlier. We also present concrete predictions on the polarization properties of the PA spectrum, which can be verified in experiments performed on oriented samples.

PACS numbers: 78.30.Jw, 78.20.Bh, 42.65.-k

## I. INTRODUCTION

Conjugated polymers have already replaced the traditional inorganic materials and emerged as popular choice for manufacturing opto-electronic devices.(**author?**)<sup>1,2,3,4</sup> The inter-molecular localized and the intra-molecular delocalized  $\pi$ -electrons are credited for the interesting linear and nonlinear optical properties in these materials. The large nonlinear optical (NLO) response in such materials is favorable for various device applications such as optical switching, computing, and electro-opto modulation.(**author?**)<sup>5,6,7</sup> These useful applications have motivated scientists to study the excited states which are important for understanding the nonlinear optics of these materials. For example, in centrosymmetric molecules, states can be classified as even parity (*gerade*) and odd parity (*ungerade*) states. From the ground state, using linear optical spectroscopy, one can probe the low-lying odd parity excited states,(**author?**)<sup>8</sup> while the even parity states stay invisible. Photo-induced absorption (PA) technique gives an opportunity to investigate these even parity states, which contribute to the nonlinear optical processes in these materials.

Among various conjugated polymers, oligo-acenes, due to their interesting electronic and optical properties, have come up as potential candidates for possible applications in the field of nonlinear optics.(**author?**)<sup>9,10</sup> Because of the alternant nature of these molecules, different states in addition to the point group symmetry ( $D_{2h}$ ) can also be classified according to their particle-hole parity ( $\pm$ ). According to normal convention, we assign the ground state  $1A_g$  a negative ( $-$ ) particle-hole parity. As per the selection rules of  $D_{2h}$  point group symmetry, for the ground-state linear optical absorption in oriented samples of oligo-acenes, two polarization channels are possible. Absorption of  $y$ -polarized photons leads the system to the  $B_{2u}^+$  manifold, while the  $x$ -polarized photons cause transitions to the  $B_{3u}^+$  states.(**author?**)<sup>8</sup> Same selection rules, therefore, also offer both these polarization possibilities for the excited state absorptions from the  $B_{2u}^+$  and  $B_{3u}^+$  states. Thus, from the  $B_{2u}^+$  type states, using  $x/y$ -polarized photons,  $B_{3g}^-/A_g^-$ -type excited states can be reached, while from the  $B_{3u}^+$  states, using  $x/y$ -polarized photons,  $A_g^-/B_{3g}^-$  can be obtained (*cf.* Fig. (1)). Here, the noteworthy point is the reverse symmetry-polarization relationship for the two types of manifolds. In the 70's, Bergman and Jortner(**author?**)<sup>11,12</sup> studied, these even parity excited states ( $A_g^-$  &  $B_{3g}^-$ ) using the two-photon absorption (TPA) spectroscopy. They measured the TPA spectra of naphthalene and anthracene in crystalline as well as in solution mode. Later, Dick and Hohlneicher measured the spectra over a wide range, between 3.59 eV to 6.20 eV for the naphthalene(**author?**)<sup>13</sup> and anthracene(**author?**)<sup>14</sup> molecules in solution. As far as the theory is concerned, the calculations have been performed using various methodologies like SDCI,(**author?**)<sup>15</sup> CASSCF,(**author?**)<sup>16,17</sup> MRMP,(**author?**)<sup>16,17</sup> LCAO-MO,(**author?**)<sup>18</sup> exact PPP,(**author?**)<sup>19,20</sup> CNDO/S-CI,<sup>21</sup> and CNDO-CI(**author?**)<sup>22</sup> on the molecular phases of these oligomers. To the best of our knowledge, none of the above mentioned calculations have reported the photo-induced absorption spectrum of any of these materials. Moreover, most of the calculations are restricted to the low-order treatment of electron-correlation effects. Therefore, in this paper, we present a large scale correlated study of photo-induced absorption spectra of the first two members of acene family, namely, naphthalene and anthracene (*cf.* Fig. (2)). The PA spectra from the  $1B_{2u}^+$  and the  $1B_{3u}^+$  states are computed, and a detailed analysis of the many-body character of the important excited states contributing to the spectra is performed. The calculations are done using the Pariser-Parr-Pople (PPP) model Hamiltonian along with full configuration interaction (FCI) technique. The standard,(**author?**)<sup>23</sup> as well as the

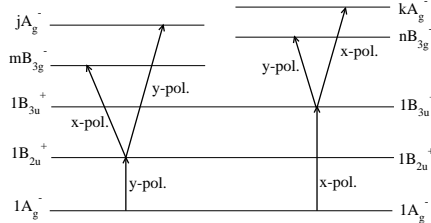


Figure 1: Schematic diagram of the essential states involved in the PA in oligoacenes, and their polarization characteristics. The arrows connecting two states imply optical absorption, with polarization directions stated next to them. Location of states is not up to scale.

screened parameters(**author?**)<sup>24</sup> are used in the PPP model Hamiltonian, and the results from both sets of calculations are compared with the experiments so as to analyze the role of Coulomb parameters. Low energy features of our calculated PA spectra match very well with the peaks observed in the two photon spectroscopy (TPS) based experiments.<sup>11,12,13,14,25</sup> Moreover, our calculations predict the presence of intense absorption features in the higher energy range of the PA spectra, along with their polarization characteristics. Particularly, for the case of anthracene novel high intensity features well below the ionization threshold should be detectable in future experiments. Predicted polarizations properties of various features can also be tested in measurements performed on oriented samples.

The remainder of this paper is organized as follows. In Sec. II we briefly review the theoretical methodology adopted in this work. In Sec. III we present and discuss our results for the photo-induced absorption from the  $1B_{2u}^+$  and the  $1B_{3u}^+$  excited states. A comparison is made with the experimental and the other available theoretical results. Finally, in Sec. IV we summarize our conclusions and provide prospects for future work.

## II. THEORY

The schematic structures of naphthalene and anthracene are shown in Fig.2. Both the molecules are assumed to lie in the  $xy$ -plane with the conjugation direction taken to be along the  $x$ -axis. The carbon-carbon bond length has been fixed at  $1.4 \text{ \AA}$ , and all bond angles have been taken to be  $120^\circ$ . The reason of choosing this symmetric geometry, as against various other possibilities has already been discussed in our earlier paper.**(author?)**<sup>8</sup> Note that these structures can also be seen as two polyene chains of suitable lengths, coupled together along the  $y$ -direction.

The correlated calculations are performed using the PPP model Hamiltonian, which can be written as

$$H = H_{C_1} + H_{C_2} + H_{C_1C_2} + H_{ee}, \quad (1)$$

where  $H_{C_1}$  and  $H_{C_2}$  are the one-electron Hamiltonians for the carbon atoms located on the



Figure 2: Schematic drawings of (a) naphthalene and (b) anthracene, considered in this work

upper and the lower polyene like chains, respectively.  $H_{C_1C_2}$  is the one-electron hopping between the two chains, and  $H_{ee}$  depicts the electron-electron repulsion. The individual terms can now be written as,

$$H_{C_1} = -t_0 \sum_{\langle k, k' \rangle} B_{k, k'}, \quad (2a)$$

$$H_{C_2} = -t_0 \sum_{\langle \mu, \nu \rangle} B_{\mu, \nu}, \quad (2b)$$

and

$$H_{C_1C_2} = -t_{\perp} \sum_{\langle k, \mu \rangle} B_{k, \mu}. \quad (2c)$$

$$H_{ee} = U \sum_i n_{i\uparrow} n_{i\downarrow} + \frac{1}{2} \sum_{i \neq j} V_{i,j} (n_i - 1)(n_j - 1) \quad (3)$$

In the equation above,  $k, k'$  are carbon atoms on the upper polyene chain,  $\mu, \nu$  are carbon atoms located on the lower polyene chain, while  $i$  and  $j$  represent all the atoms of the oligomer. Symbol  $\langle \dots \rangle$  implies nearest neighbors, and  $B_{i,j} = \sum_{\sigma} (c_{i,\sigma}^{\dagger} c_{j,\sigma} + h.c.)$ . Matrix elements  $t_0$ , and  $t_{\perp}$  depict one-electron hops. As far as the values of the hopping matrix elements are concerned, we took  $t_0 = 2.4$  eV for both intracell and intercell hopping, and  $t_{\perp} = t_0$  consistent with the undimerized ground state for polyacene argued by Raghu *et al.*<sup>(author?)</sup><sup>26</sup>

The Coulomb interactions are parametrized according to the Ohno relationship,<sup>(author?)</sup><sup>23</sup>

$$V_{i,j} = U / \kappa_{i,j} (1 + 0.6117 R_{i,j}^2)^{1/2}, \quad (4)$$

where,  $\kappa_{i,j}$  depicts the dielectric constant of the system which can simulate the effects of screening,  $U$  is the on-site repulsion term, and  $R_{i,j}$  is the distance in Å between the  $i$ th carbon and the  $j$ th carbon. In the present work, we have performed calculations using “standard parameters”<sup>23</sup> with  $U = 11.13$  eV and  $\kappa_{i,j} = 1.0$ , as well as “screened parameters”<sup>24</sup> with  $U = 8.0$  eV and  $\kappa_{i,j} = 2.0$  ( $i \neq j$ ) and  $\kappa_{i,i} = 1.0$ . The screened parameters employed here were devised by Chandross and Mazumdar<sup>24</sup> with the aim of accounting for the interchain screening effects in phenylene based polymers. Our motive behind using these parameters is precisely the same.

The starting point of the correlated calculations for the molecules are the restricted Hartree-Fock (HF) calculations, using the PPP Hamiltonian. The many-body effects beyond HF are computed using the full configuration interaction (FCI) method. Details of this CI-based many-body procedures have been presented in our earlier works.<sup>(author?)</sup><sup>27, 28, 29, 30</sup>

From the CI calculations, we obtain the eigenfunctions and eigenvalues corresponding to the correlated ground and excited states of examined molecules. Using these eigenfunctions the dipole matrix elements amongst various excited states are computed. These dipole matrix elements, along with the energies of the excited states are, in turn, utilized to calculate various PA spectra. The number of excited states computed for each symmetry manifold is quite large, ranging typically from 70–100, allowing us to probe a broad energy range in the PA spectrum.

### III. RESULTS AND DISCUSSION

In this section, we discuss our FCI results on the PA spectrum of naphthalene and anthracene. Fig. (3 and 4) presents the PA spectra of naphthalene and anthracene, respectively. The spectra are computed using the standard (left panel) as well as the screened parameters (right panel) in the PPP Hamiltonian. For both  $1B_{2u}^+$  and  $1B_{3u}^+$  excited state absorption, we present the  $x$ - and  $y$ -polarized spectra separately, so as to facilitate comparison with experiments performed on oriented samples. The wave functions of the excited states contributing to various peaks in spectra are tabulated in tables (*cf.* Ref.<sup>31</sup>). Since, the calculations are performed using the FCI approach, they are exact within the model chosen and cannot be improved. Therefore, any discrepancy which these results may exhibit with respect to the experiments is a reflection of the limitations of the model or the parameters used, and not that of the correlation approach. At this point, we would like to note that Ramasesha and coworkers have also presented FCI results on naphthalene<sup>19,32</sup> and anthracene.<sup>20,32</sup> However, for the case of naphthalene they only presented the energies of some of the low-lying states, but did not calculate transition dipoles. While, for anthracene they computed the transition dipoles among a few even and odd parity states, but the PA spectrum was not probed. Moreover, the energy range of the states computed by us extends higher than the calculations performed earlier, and therefore, can be used to interpret future experiments.

In our earlier paper,<sup>8</sup> we showed that experiments as well as calculations suggest that for both the oligomers  $1B_{3u}^+$  state is located at least 1.5 eV higher than  $1B_{2u}^+$  state. Therefore if in a PA experiment, the pump is tuned close to  $1B_{2u}^+$  energy, using an appropriate probe beam one can investigate higher excited states which are dipole connected to  $1B_{2u}^+$ . Thus, we will measure excited state absorptions only from the  $1B_{2u}^+$  state, without any intermixing from  $1B_{3u}^+$  PA spectrum. Moreover, employing oriented samples, individual energy manifolds ( $A_g^-/B_{3g}^-$ ) can be investigated by using  $x$ - or  $y$ -polarized probe beams. Similarly, one can measure the  $1B_{3u}^+$  excited state absorption by tuning the pump energy to  $E(1B_{3u}^+)$ . Therefore, by choosing suitable pump energies and oriented samples, all the four components of the PA spectrum of each oligomer computed here, can be measured separately. We would like to mention here that  $1B_{2u}^+$  and  $1B_{3u}^+$  PA spectra are plotted with respect to their energies obtained in linear optical spectra, reported in Ref. (<sup>8</sup>). In naphthalene, using standard parameters we calculated  $1B_{2u}^+$  state at 4.45 eV and  $1B_{3u}^+$  state at 5.99 eV, while screened parameter values for these states were obtained to be 4.51 eV and 5.30 eV, respectively. In case of anthracene, standard parameters predicted  $E(1B_{2u}^+) = 3.66$  eV and  $E(1B_{3u}^+) = 5.34$  eV, on the other hand screened parameters calculated  $1B_{2u}^+$  and  $1B_{3u}^+$  states at 3.55 eV and 4.64 eV, respectively. The energies reported in tables (*cf.* Ref.<sup>31</sup>) are the excitation energies of those states calculated with respect to the  $1A_g^-$  ground state.

We first present the lower end of the spectrum, which is that region where experimental

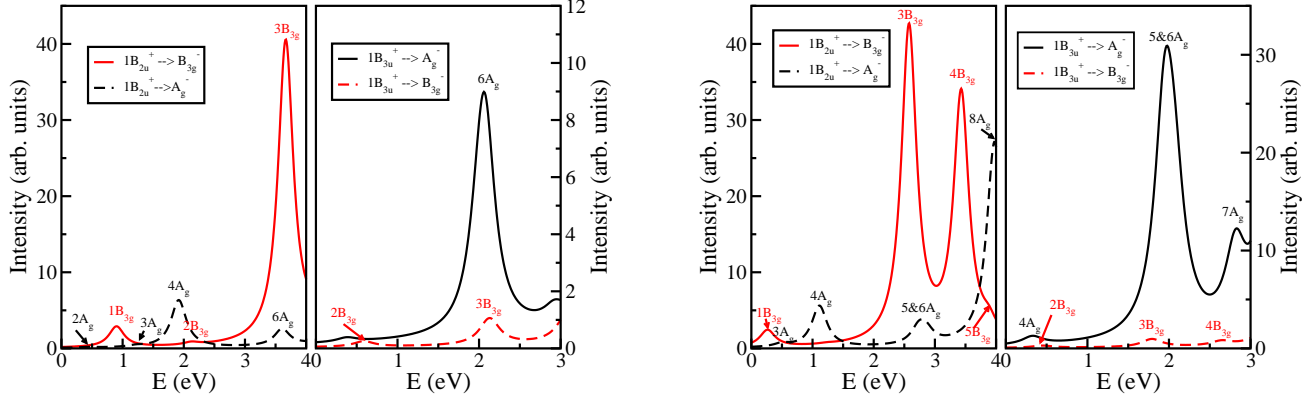


Figure 3: (color online) Photo-induced spectra of naphthalene computed using standard parameters (left panel) and screened parameters (right panel) in the PPP model Hamiltonian. The left side of both the spectrum depicts the PA from the  $1B_{2u}^+$  state, while right side shows it from the  $1B_{3u}^+$  state. The  $x(y)$ -polarized transitions are shown using solid (dashed) curves.

information about various excited states is available through two photon spectroscopy based experiments.<sup>11,12,13,14,25</sup> Although, the energies of these states are not so low in terms of their absolute values, but these states will appear in the low energy region of the PA spectrum. In absolute terms, the states for naphthalene and anthracene in this region are up to 6.5 eV and 5.2 eV, respectively, while in the PA spectra, they will appear in the range of 0–2 eV for naphthalene, and 0–1.6 eV for anthracene. Thereafter, we compare our results with the experimental data and calculations of other authors. Next, we present the discussion for the higher energy region of the spectrum which so far has not been probed, either experimentally, or theoretically. While discussing the high energy features we have to keep in mind that the ionization potentials of naphthalene and anthracene are 8.1 eV and 7.4 eV, respectively.

### A. Low energy region of the PA spectrum

The first general aspect of the calculation is the relative location of the  $2A_g^-$  state of these oligomers with respect to their  $1B_{2u}^+$  state. Experimentally speaking both naphthalene and anthracene exhibit fluorescence, suggesting that  $1B_{2u}^+$  state is lower than  $2A_g^-$  state. In our standard parameter calculations we obtain this ordering of states, while in screened parameter calculation  $2A_g^-$  state is obtained below  $1B_{2u}^+$  state. As a result,  $2A_g^-$  state does not appear in the  $1B_{2u}^+$  PA spectrum, computed using the screened parameters, while in standard parameter spectrum it appears as the first (but very weak) feature in both the molecules (*cf.* left panel of Fig. (3) and Fig. (4)). After the  $2A_g^-$  peak, the next important feature in the spectra corresponds to the  $1B_{3g}^-$  state, which is relatively more intense than the  $2A_g^-$  feature. The intensity of the  $1B_{3g}^-$  peak increases, while that of  $2A_g^-$  decreases, with the increase in length of molecule, irrespective of the parameters used. Both features occur due to transition from the  $1B_{2u}^+$  state. Turning over to the  $1B_{3u}^+$  PA spectra, we notice that the low energy region gets very faint contributions from some of the states which contribute to the intermediate energy region of  $1B_{2u}^+$  PA spectra.

Now we compare our results for naphthalene and anthracene with the experiments, and the works of other authors in a quantitative manner. For both the oligomers, this comparison

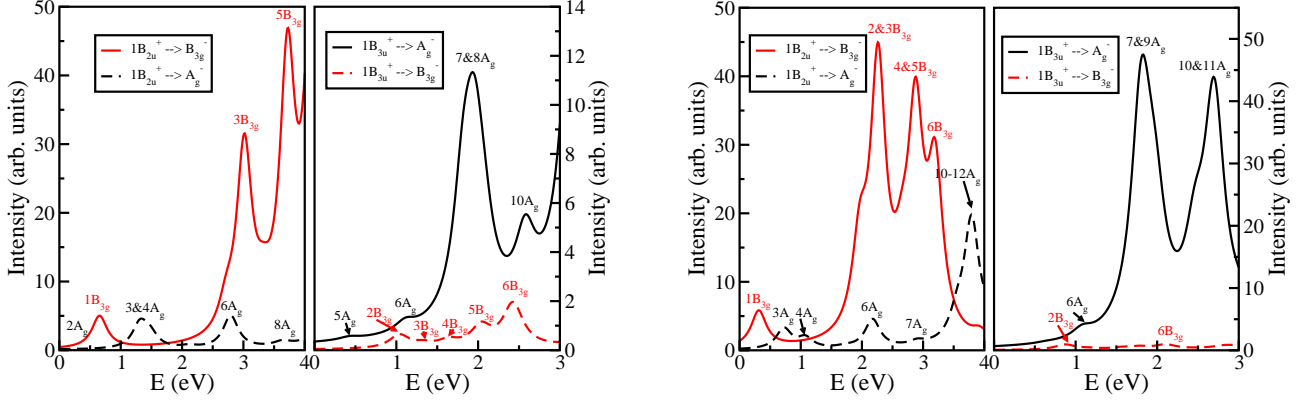


Figure 4: (color online) Photo-induced spectra of anthracene computed using standard parameters (left panel) and screened parameters (right panel) in the PPP model Hamiltonian. The left side of both the spectrum depicts the PA from the  $1B_{2u}^+$  state, while right side shows it from the  $1B_{3u}^+$  state. The  $x/y$ -polarized transitions are shown using solid/dashed curves.

is summarized in Table I. For the case of naphthalene, our results obtained using the standard parameters are in very good agreement with the available experimental and other theoretical results, while screened parameters underestimate the experimental findings (*cf.* Table I). Our standard parameter calculations predict a very weak peak corresponding to  $2A_g^-$  state at 4.91 eV, while  $1B_{3g}^-$ ,  $3A_g^-$ , and  $4A_g^-$  states are obtained at 5.35 eV, 5.67 eV, and 6.37 eV, respectively. Upon comparing our results to experiments, we find that the measured energy (author?)<sup>11, 13, 25</sup> of the  $2A_g^-$  &  $3A_g^-$  states ( $\approx 5.50$  eV & 6.05 eV) compares very well with our computed energy for  $3A_g^-$  and  $4A_g^-$  states (5.67 eV & 6.37 eV). Thus, the measured  $nA_g^-$  state consequently maps to  $(n+1)A_g^-$  state of our work. We strongly believe that the  $2A_g^-$  state located around 4.91 eV ( $\approx 39601$   $\text{cm}^{-1}$ ) has been missed by the experimentalists due to its very weak intensity. This, in our opinion calls for further experimental investigations. While comparing theory and experiments for the anthracene, a similar mismatch in the labeling of the  $A_g^-$  states was pointed out by Ramasesha *et al.* (author?)<sup>20</sup> On the other hand, there is no ambiguity for the  $1B_{3g}^-$  state, which is calculated at 5.35 eV by us and measured around 5.20 eV, using two photon spectroscopy (TPS). (author?)<sup>11, 13, 25</sup> Thus, the disagreement between our theory and experiments is no more than 5%. When this  $nA_g^- - (n+1)A_g^-$  mismatch is accounted for, we obtain very good agreement between our calculations and those of Hohlneicher and Dick, (author?)<sup>22</sup> who reported  $1B_{3g}^-$ ,  $2A_g^-$ , and  $3A_g^-$  states at 5.31 eV, 5.45 eV, and 5.91 eV using SDCl/M approach, and at 5.37 eV, 5.70 eV, and 6.12 eV using SDCl/P approach. Our results also agree well with the CNDO/S-CI calculations of Swiderek *et al.*, (author?)<sup>21</sup> who computed  $1B_{3g}^-$ ,  $2A_g^-$ , and  $3A_g^-$  states at 5.37 eV, 5.61 eV, and 5.76 eV, respectively. On comparing our results with the MRMP and CASSCF calculations of Hashimoto *et al.*, (author?)<sup>16</sup> we found that their CASSCF energies are much higher than ours, as well as compared to experimental energies, while MRMP results are comparable. Similarly, SCI results of Pariser (author?)<sup>18</sup> predict much higher energies differences as compared to our values.

In anthracene, the standard parameters predict  $2A_g^-$ ,  $1B_{3g}^-$ ,  $3A_g^-$ , and  $4A_g^-$  states at 3.89 eV, 4.31 eV, 4.98 eV, and 5.14 eV, respectively, while the screened parameters values for the  $1B_{3g}^-$ ,  $3A_g^-$ , and  $4A_g^-$  states are 3.86 eV, 4.28 eV, and 4.61 eV, respectively. In order to compare our results with the two photon excitation spectrum measured by Dick and

Hohlneicher, (author?)<sup>13</sup> we found that they reported a very weak intensity peak around 3.64 eV ( $\approx 29300 \text{ cm}^{-1}$ ) and associated  $A_g^-$  symmetry to it. Although, they did not assign any state to this feature, yet from our computed PA spectrum and excitation energy it compares very favorably with calculated  $2A_g^-$  state, a fact also noted by Ramasesha *et al.* (author?)<sup>20</sup> Therefore, following the lead of Ramasesha *et al.* (author?)<sup>20</sup>, we also compare experimental  $nA_g$  states with our  $(n+1)A_g$  states. This brings our standard parameters results in very good agreement with the experimental values of Dick and Hohlneicher, who reported  $1B_{3g}^-$ ,  $2A_g^-$ , and  $3A_g^-$  states at 4.44 eV, 4.71 eV, and 5.33 eV, respectively. (author?)<sup>14</sup> Prior to Dick and Hohlneicher (author?)<sup>14</sup>, Bergman and Jortner (author?)<sup>12</sup> also measured the two photon spectrum of anthracene molecule in solution, as well as of crystalline anthracene. As is obvious from Table I that our standard parameter values are in good agreement with both their data. Since screened parameter results consistently underestimate the experimental values, we believe that they are not applicable for the case of anthracene as well. As far as comparison with other theoretical work is concerned, understandably our results are in excellent agreement with the work of Ramasesha *et al.* (author?)<sup>20</sup> who also used the FCI method in conjunction with the PPP model Hamiltonian. However, we have gone beyond the work of Ramasesha *et al.* (author?)<sup>20</sup> by also calculating the PA spectra of anthracene. On comparing our  $(n+1)A_g$  states with the  $nA_g$  states predicted by Kawashima *et al.*,<sup>17</sup> we obtain a very good agreement with the MRMP calculations. The calculations performed by other authors using SDCI/M, (author?)<sup>22</sup> SDCI/P, (author?)<sup>22</sup> CASSCF, (author?)<sup>17</sup> and SCI, (author?)<sup>18</sup> approaches predict the states discussed at relatively larger energies than our results.

## B. Higher energy region of the PA spectrum

This higher energy region, which includes the excited states in the range 6.6 eV to 8.1 eV for naphthalene, and 5.3 eV to 7.4 eV for anthracene, has so far not been experimentally explored. In this region of the PA spectra highest intensity transitions correspond to the  $x$ -polarized photons, in agreement with the fact that the conjugation length of the systems is in the  $x$ -direction. Therefore,  $B_{3g}^-$  states lead to the most intense peaks in the  $1B_{2u}^+$  PA spectra, while  $A_g^-$  states contribute to the main intensity of the  $1B_{3u}^+$  PA spectra. However, when these two  $x$ -polarized transitions are compared to each other,  $B_{3g}^-$  peaks are found to be more intense than  $A_g^-$  peaks. Thus,  $B_{3g}^-$  states which exhibit strong dipole coupling to  $1B_{2u}^+$  may end up playing the same role in the nonlinear properties of these materials which the  $mA_g^-$  state plays for *trans*-polyacetylene.<sup>33,34</sup>

For naphthalene, with standard parameters  $2B_{3g}^-$  state (6.58 eV) leads to low intensity features (*cf.* Fig. 3), while the  $3B_{3g}^-$  state (8.1 eV) close to the ionization threshold leads to a very intense peak in  $1B_{2u}^+$  PA spectrum. Similarly,  $6A_g^-$  (8.06 eV) also located close to the ionization threshold contributes a very intense peak to the  $1B_{3u}^+$  PA spectrum and a weak one to the  $1B_{2u}^+$  spectrum. Because of its proximity to the ionization threshold it may be difficult to detect the  $6A_g^-$  and  $3B_{3g}^-$  states, but the  $2B_{3g}^+$  state should certainly be detectable.

The PA spectrum of anthracene computed using the standard parameters is much richer compared to that of naphthalene, and offers many more detectable peaks. For example, in the  $B_{3g}^-$  manifold, states  $2B_{3g}^-$  (6.37 eV),  $3B_{3g}^-$  (6.68 eV), and  $4B_{3g}^-$  (6.98 eV), are well below the ionization threshold of 7.4 eV and lead to significant peaks either in the  $1B_{2u}^+$  or  $1B_{3u}^+$



PA spectra. Particularly noteworthy is the strong intensity of the  $3B_{3g}^-$  peak in the  $1B_{2u}^+$  PA spectrum.  $5B_{3g}^-$  state at 7.39 eV also leads to an intense peak but may be difficult to detect because of its closeness to the ionization threshold. As far as the  $A_g^-$  manifold is concerned,  $5A_g^-$  (5.77 eV),  $6A_g^-$  (6.45 eV), and  $7A_g^-$  (7.16 eV) states contribute significant intensity to the PA spectrum and have not been explored so far. Reasonably strong intensities, coupled with the fact that they are away from the ionization threshold makes them strong candidates for experimental investigation. The  $8A_g^-$  (7.3 eV) peak which is also quite intense is close to the ionization threshold and hence may be difficult to detect.

As far as the screened parameters based results are concerned, for both the oligomers more features are visible in the same energy range, because of the fact that the spectrum is red shifted as compared to the standard parameters. This trend is in agreement with our earlier work on linear optical absorption in these materials.<sup>8</sup> For example, in naphthalene states all the way up to  $4B_{3g}^-$  and  $7A_g^-$ , while for anthracene states up to  $6B_{3g}^-$  and  $11A_g^-$ , are below the ionization threshold of individual oligomers, and therefore, in principle are detectable. Thus, the experimental investigation of these high energy features can throw light on the nature of Coulomb interactions in these materials. Smaller number of peaks below the ionization threshold will indicate that the standard parameters describe the Coulomb interactions in these systems, while the larger number of features will suggest the validity of the screened parameters.

Regarding wave functions, one can notice from the tables (*cf.* Ref.<sup>31</sup>), that single as well as double excitations contribute equally to various excited states visible in these spectra. In particular, the main configuration contributing to the many-particle wave function of the  $2A_g^-$  state corresponds to a double excitation described by HOMO ( $H$ ) $\rightarrow$ LUMO ( $L$ ); HOMO ( $H$ ) $\rightarrow$ LUMO ( $L$ ) ( $|H \rightarrow L; H \rightarrow L\rangle$ ), while single excitation  $|H \rightarrow L + 2\rangle \pm c.c.$  is found as the major contributor to the many-particle wave function of the  $1B_{3g}^-$  state. The most intense  $B_{3g}^-$  feature for both naphthalene and anthracene computed using the standard as well as the screened parameter occurs mainly due to  $|H \rightarrow L; H \rightarrow L + 1\rangle \pm c.c.$  excitation. For the case of  $A_g^-$  peaks, maximum intensity can be attributed to states which for both the oligomers, and irrespective of parameters used, are described by  $|H \rightarrow L; H - 1 \rightarrow L + 1\rangle$  configuration.

#### IV. CONCLUSIONS

In this paper, we presented FCI method based large scale correlated calculations of photo-induced absorption spectrum of naphthalene and anthracene from their low-lying one-photon states,  $1B_{2u}^+$  and  $1B_{3u}^+$ . The aim behind these calculations was to understand the nature of important two photon states of these materials and their coupling to one photon states. The spectra were computed over a broad energy range, so far unexplored in earlier calculations as well as experiments. The main conclusions of this work are as follows:

1. Our most reliable results were obtained using standard Coulomb parameters in the Hamiltonian, leading to excellent agreement on the energies of low lying two photon states, available from two photon spectroscopy (TPS) experiments.
2. In particular, the  $2A_g^-$  state was calculated to be higher than the  $1B_{2u}^+$  state, predicting these materials to exhibit fluorescence, in agreement with experimental data. However, two photon spectroscopy based experiments have not been able to locate the  $2A_g^-$  state,

Table I: Comparison of results of our calculations performed with the standard (Std.) parameters and the screened (Scd.) parameters with other experimental and theoretical results for the most important low-lying even parity states. The energies of various states are given with respect to the ground state ( $1A_g^-$ ). In naphthalene and anthracene, using the standard parameters  $1B_{2u}^+$  state was obtained at 4.45 eV and 3.66 eV, respectively.<sup>8</sup> The screened parameters predicted  $1B_{2u}^+$  at 4.51 eV for naphthalene, and 3.55 eV for anthracene.<sup>8</sup>

State	Present work		Experimental	Other theoretical		Excitation energy (eV)	
	Std.	Scd.		-	-	-	-
	para.	para.					
Naphthalene (C <sub>10</sub> H <sub>8</sub> )							
$2A_g^-$	4.91	-	-	-	-	-	-
$1B_{3g}^-$	5.35	4.77	5.22,(author?) <sup>13</sup>	5.21,(author?) <sup>11</sup>	5.27(author?) <sup>25</sup>	5.31 <sup>a</sup> ,(author?) <sup>22</sup>	5.37 <sup>b</sup> ,(author?) <sup>22</sup>
$3A_g^-$	5.67	5.01	5.52,(author?) <sup>13</sup>	5.45,(author?) <sup>11</sup>	5.50(author?) <sup>25</sup>	5.45 <sup>a</sup> ,(author?) <sup>22</sup>	5.70 <sup>b</sup> ,(author?) <sup>22</sup>
$4A_g^-$	6.37	5.62	6.05(author?) <sup>13</sup>		-	5.91 <sup>a</sup> ,(author?) <sup>22</sup>	6.12 <sup>b</sup> ,(author?) <sup>22</sup>
Anthracene (C <sub>14</sub> H <sub>10</sub> )							
$2A_g^-$	3.89	-	3.64 <sup>e</sup> (author?) <sup>14</sup>		-	-	-
$1B_{3g}^-$	4.31	3.86	4.44 <sup>e</sup> ,(author?) <sup>14</sup>	4.53 <sup>f</sup> ,(author?) <sup>12</sup>	4.66 <sup>e</sup> ,(author?) <sup>12</sup>	4.31,(author?) <sup>20</sup>	4.57 <sup>a</sup> ,(author?) <sup>20</sup>
$3A_g^-$	4.98	4.28	4.71 <sup>e</sup> ,(author?) <sup>14</sup>	4.81 <sup>f</sup> ,(author?) <sup>12</sup>	4.96 <sup>e</sup> ,(author?) <sup>12</sup>	4.96,(author?) <sup>20</sup>	4.29 <sup>a</sup> ,(author?) <sup>20</sup>
$4A_g^-$	5.14	4.61	5.33 <sup>e</sup> (author?) <sup>14</sup>		-	5.12,(author?) <sup>20</sup>	5.18 <sup>a</sup> ,(author?) <sup>20</sup>

<sup>a</sup>SDCI/M calculations

<sup>d</sup>CASSCF calculations

<sup>b</sup>SDCI/P calculations

<sup>e</sup>solution spectrum

<sup>c</sup>MRMP calculations

<sup>f</sup>crystalline spectrum

possibly due to its very low intensity. Therefore, we encourage careful TPS or PA based measurements of the  $2A_g^-$  state in these materials to verify our predictions.

3. We make specific predictions about the higher energy region of the PA spectra, where we found intense features corresponding both to the  $A_g^-$  and  $B_{3g}^-$  type states. These states may also be visible in the TPS experiments in the higher energy region, which so far has not been explored. We further predict that the relative intensities of the peaks corresponding to  $x$ -polarized transitions is more than the  $y$ -polarized ones, which can be probed in experiments performed with the oriented samples.
4. We believe that it is feasible to resolve various components of the PA spectra computed here, by tuning the pump beam to different energies ( $E(1B_{2u}^+)$  or  $E(1B_{3u}^+)$ ), and by using oriented samples.

Because of all the reasons mentioned above it is of interest to probe the PA spectra of these well established materials; therefore, we urge strong experimental efforts in this direction.

The calculation of TPA spectrum will additionally verify our results, as the peaks appearing in the PA spectra should also appear in the TPA spectra of the considered oligomers. Moreover, some of the important features of the PA spectra may also appear in the third harmonic generation (THG) spectra, giving more insight into the states governing the non-linear optics of these materials. Therefore, in near future we will present the results of calculations of the TPA and THG spectra of oligo-acenes, which are currently underway in our group.

## Acknowledgments

We thank the Department of Science and Technology (DST), Government of India, for providing financial support for this work under Grant No. SR/S2/CMP-13/2006.

- 
- <sup>1</sup> M. A. Baldo, M. E. Thompson, and S. R. Forrest, *Nature* **403**, 750 (2000).
  - <sup>2</sup> S. R. Forrest, *Nature* **428**, 911 (2004).
  - <sup>3</sup> G. Malliaras and R. Friend, *Phys. Today* **58**, No. 5, 53 (2005).
  - <sup>4</sup> M. E. Gershenson, V. Podzorov, and A. F. Morpurgo, *Rev. Mod. Phys.* **78**, 973 (2006).
  - <sup>5</sup> R. W. Eason and A. Miller, *Nonlinear Optics in Signal Processing*, Chapman & Hall, London (1993).
  - <sup>6</sup> J. Zyss, *Molecular Nonlinear Optics: Materials, Physics, and Devices*, Academic Press Boston, MA (1994).
  - <sup>7</sup> J. L. Bredas, C. Adant, P. Tackx, and A. Persoons, *Chem. Rev.* **94**, 243 (1994).
  - <sup>8</sup> P. Sony and A. Shukla, *Phys. Rev. B* **75**, 155208 (2007).
  - <sup>9</sup> C. D. Dimitrakopoulos and P.R. L. Malenfant, *Adv. Mater.* **14**, 99 (2002).
  - <sup>10</sup> E. M. Muller and J. A. Marohn, *Adv. Mater.* **17**, 1410 (2005).
  - <sup>11</sup> A. Bergman and J. Jortner, *Chem. Phys. Lett.* **26**, 323 (1974).
  - <sup>12</sup> A. Bergman and J. Jortner, *Chem. Phys. Lett.* **15**, 309 (1972).
  - <sup>13</sup> B. Dick and G. Hohlneicher, *Chem. Phys. Lett.* **84**, 471 (1981).
  - <sup>14</sup> B. Dick and G. Hohlneicher, *Chem. Phys. Lett.* **83**, 615 (1981).
  - <sup>15</sup> P. Tavan and K. Schulten, *J. Chem. Phys.* **70**, 5414 (1979).
  - <sup>16</sup> T. Hashimoto, H. Nakano, and K. Hirao, *J. Chem. Phys.* **104**, 6244 (1996).
  - <sup>17</sup> Y. Kawashima, T. Hashimoto, H. Nakano, and K. Hirao, *Theor. Chem. Acc* **102**, 49 (1999).
  - <sup>18</sup> R. Pariser, *J. Chem. Phys.* **24**, 250 (1956).
  - <sup>19</sup> S. Ramasesha and Z. G. Soos, *Chem. Phys.* **91**, 35 (1984).
  - <sup>20</sup> S. Ramasesha, D. S. Galvão, and Z. G. Soos, *J. Phys. Chem.* **97**, 2823 (1993).
  - <sup>21</sup> P. Swiderek, M. Michaad, G. Hohlneicher, and L. Sanche, *Chem. Phys. Lett.* **175**, 667 (1990).
  - <sup>22</sup> G. Hohlneicher and B. Dick, *J. Chem. Phys.* **70**, 5427 (1979).
  - <sup>23</sup> K. Ohno, *Theor. Chim. Acta* **2**, 219 (1964).
  - <sup>24</sup> M. Chandross and S. Mazumdar, *Phys. Rev. B* **55**, 1497 (1997).
  - <sup>25</sup> N. Mikami and M. Ito, *Chem. Phys. Lett.* **31**, 472 (1975).
  - <sup>26</sup> C. Raghu, Y. Anusooya Pati, and S. Ramasesha, *Phys. Rev. B* **65**, 155204 (2002).
  - <sup>27</sup> H. Ghosh, A. Shukla, and S. Mazumdar, *Phys. Rev. B* **62**, 12763 (2000).
  - <sup>28</sup> A. Shukla, *Phys. Rev. B* **65**, 125204 (2002).
  - <sup>29</sup> A. Shukla, *Chem. Phys.* **300**, 177 (2004).
  - <sup>30</sup> A. Shukla, *Phys. Rev. B* **69**, 165218 (2004).
  - <sup>31</sup> Attached as an EPAPS document.
  - <sup>32</sup> C. Raghu, Y. Anusooya Pati, and S. Ramasesha, *Phys. Rev. B* **66**, 035116 (2002).
  - <sup>33</sup> S. N. Dixit, D. Guo, and S. Mazumdar, *Phys. Rev. B* **43**, 6781 (1991).
  - <sup>34</sup> S. Mazumdar and F. Guo, *J. Chem. Phys.* **100**, 1665 (1994).

# SUPPLEMENTARY INFORMATION

Here we present the tables summarizing the results of our FCI calculations for excited state absorption in naphthalene and anthracene. The data presented in the tables includes important configurations contributing to the many-body wave functions of various excited states, their excitation energies, and transition dipoles connecting them to the  $1B_{2u}^+$  state and  $1B_{3u}^+$  state.

## A. Naphthalene

Table II:  $A_g^-$ -type excited states contributing to the photo-induced absorption spectrum of naphthalene, corresponding to transition from  $1B_{2u}^+$  (at 4.45 eV) and  $1B_{3u}^+$  state (at 5.99 eV) due to the absorption of  $y$ -polarized and  $x$ -polarized photons, respectively, computed using the FCI method coupled with the standard parameters in the PPP model Hamiltonian. The table includes many particle wave functions, excitation energies, and dipole matrix elements of various states with respect to  $1B_{2u}^+$  and  $1B_{3u}^+$  states. ‘+c.c.’ indicates that the coefficient of charge conjugate of a given configuration has the same sign, while ‘-c.c.’ implies that the two coefficients have opposite signs.

State	E (eV)	Transition		Wave Functions
		$y$ -component	$x$ -component	
$2A_g^-$	4.91	0.162	-	$ H - 2 \rightarrow L + 1\rangle + c.c.(0.4120)$
				$ H \rightarrow L; H \rightarrow L\rangle (0.4047)$
				$ H \rightarrow L + 3\rangle + c.c.(0.3555)$
$3A_g^-$	5.67	0.147	-	$ H \rightarrow L; H - 1 \rightarrow L + 1\rangle (0.4062)$
				$ H - 1 \rightarrow L + 2\rangle - c.c.(0.3918)$
				$ H \rightarrow L + 3\rangle + c.c.(0.3253)$
$4A_g^-$	6.37	0.697	0.242	$ H \rightarrow L; H \rightarrow L\rangle (0.2196)$
				$ H \rightarrow L; H - 2 \rightarrow L + 2\rangle (0.2732)$
				$ H \rightarrow L; H - 1 \rightarrow L + 1\rangle (0.2556)$
$6A_g^-$	8.06	0.300	0.734	$ H \rightarrow L + 2; H \rightarrow L + 2\rangle + c.c.(0.2537)$
				$ H \rightarrow L; H - 1 \rightarrow L + 1\rangle (0.4981)$
				$ H \rightarrow L; H - 2 \rightarrow L + 2\rangle (0.3886)$
				$ H \rightarrow L + 2; H \rightarrow L + 2\rangle + c.c.(0.2912)$
				$ H - 2 \rightarrow L + 4\rangle + c.c.(0.2143)$

Table III:  $B_{3g}^-$ -type excited states contributing to the photo-induced absorption spectrum of naphthalene, corresponding to transition from  $1B_{2u}^+$  (at 4.45 eV) and  $1B_{3u}^+$  state (at 5.99 eV) due to the absorption of  $x$ -polarized and  $y$ -polarized photons, respectively, computed using the FCI method coupled with the standard parameters in the PPP model Hamiltonian. The table includes many particle wave functions, excitation energies, and dipole matrix elements of various states with respect to  $1B_{2u}^+$  and  $1B_{3u}^+$  states. ‘+c.c.’ indicates that the coefficient of charge conjugate of a given configuration has the same sign, while ‘-c.c.’ implies that the two coefficients have opposite signs.

State	E (eV)	Transition	Dipole (Å)	Wave Functions
		$x$ -component	$y$ -component	
$1B_{3g}^-$	5.35	0.672	-	$ H \rightarrow L + 2\rangle + c.c.(0.5469)$
				$ H \rightarrow L; H \rightarrow L + 1\rangle + c.c.(0.2841)$
$2B_{3g}^-$	6.58	0.154	0.219	$ H - 1 \rightarrow L + 3\rangle + c.c.(0.4828)$
				$ H - 1 \rightarrow L + 1; H \rightarrow L + 1\rangle + c.c.(0.3665)$
$3B_{3g}^-$	8.12	1.271	0.255	$ H \rightarrow L; H \rightarrow L + 1\rangle + c.c.(0.4081)$
				$ H \rightarrow L + 2\rangle + c.c.(0.2349)$
				$ H \rightarrow L; H \rightarrow L + 4\rangle + c.c.(0.2335)$
				$ H - 3 \rightarrow L; H \rightarrow L + 2\rangle + c.c.(0.2256)$
				$ H - 2 \rightarrow L\rangle + c.c.(0.2128)$

Table IV:  $A_g^-$ -type excited states contributing to the photo-induced absorption spectrum of naphthalene, corresponding to transition from  $1B_{2u}^+$  (at 4.51 eV) and  $1B_{3u}^+$  state (at 5.30 eV) due to the absorption of  $y$ -polarized and  $x$ -polarized photons, respectively, computed using the FCI method coupled with the screened parameters in the PPP model Hamiltonian. The table includes many particle wave functions, excitation energies, and dipole matrix elements of various states with respect to  $1B_{2u}^+$  and  $1B_{3u}^+$  states. ‘+c.c.’ indicates that the coefficient of charge conjugate of a given configuration has the same sign, while ‘-c.c.’ implies that the two coefficients have opposite signs.

State	E (eV)	Transition	Dipole (Å)	Wave Functions
		$y$ -component	$x$ -component	
$3A_g^-$	5.01	0.355	-	$ H \rightarrow L; H - 1 \rightarrow L + 1\rangle (0.4022)$
				$ H \rightarrow L + 3\rangle - c.c.(0.3582)$
				$ H - 1 \rightarrow L + 2\rangle + c.c.(0.3396)$
$4A_g^-$	5.62	0.856	0.612	$ H \rightarrow L; H \rightarrow L\rangle (0.5903)$

Continued on next page

Table IV – continued from previous page

State	E (eV)	Transition		Dipole (Å)	Wave Functions
		<i>y</i> -component	<i>x</i> -component		
					$ H \rightarrow L; H - 2 \rightarrow L + 2\rangle$ (0.2873)
					$ H - 1 \rightarrow L + 2\rangle + c.c.$ (0.2594)
					$ H \rightarrow L + 2; H \rightarrow L + 2\rangle - c.c.$ (0.2494)
$5A_g^-$	7.25	0.336	1.331		$ H \rightarrow L; H - 1 \rightarrow L + 1\rangle$ (0.5808)
					$ H \rightarrow L + 1; H \rightarrow L + 1\rangle - c.c.$ (0.3109)
$6A_g^-$		-	0.872		$ H \rightarrow L; H - 1 \rightarrow L + 1\rangle$ (0.3260)
					$ H - 2 \rightarrow L + 4\rangle + c.c.$ (0.3156)
					$ H \rightarrow L; H - 2 \rightarrow L + 2\rangle$ (0.2960)
					$ H \rightarrow L + 2; H \rightarrow L + 2\rangle - c.c.$ (0.2204)
$7A_g^-$	8.13	-	0.657		$ H - 4 \rightarrow L + 2\rangle + c.c.$ (0.2293)
					$ H \rightarrow L; H - 1 \rightarrow L + 1\rangle$ (0.2262)
$8A_g^-$	8.48	0.978	0.817		$ H - 1 \rightarrow L + 1; H - 1 \rightarrow L + 1\rangle$ (0.3318)
					$ H - 2 \rightarrow L + 2; H - 1 \rightarrow L + 1\rangle$ (0.2959)
					$ H \rightarrow L; H - 1 \rightarrow L + 1\rangle$ (0.4022)
					$ H \rightarrow L + 3\rangle - c.c.$ (0.2825)

Table V:  $B_{3g}^-$ -type excited states contributing to the photo-induced absorption spectrum of naphthalene, corresponding to transition from  $1B_{2u}^+$  (at 4.51 eV) and  $1B_{3u}^+$  (at 5.30 eV) states due to the absorption of *x*-polarized and *y*-polarized photons, respectively, computed using the FCI method coupled with the screened parameters in the PPP model Hamiltonian. The table includes many particle wave functions, excitation energies, and dipole matrix elements of various states with respect to  $1B_{2u}^+$  and  $1B_{3u}^+$  states. ‘+c.c.’ indicates that the coefficient of charge conjugate of a given configuration has the same sign, while ‘-c.c.’ implies that the two coefficients have opposite signs.

State	E (eV)	Transition		Dipole (Å)	Wave Functions
		<i>x</i> -component	<i>y</i> -component		
$1B_{3g}^-$	4.77	1.119	-		$ H \rightarrow L + 2\rangle + c.c.$ (0.5519)
					$ H \rightarrow L; H \rightarrow L + 1\rangle - c.c.$ (0.2247)
$2B_{3g}^-$	5.75	-	0.263		$ H - 1 \rightarrow L + 3\rangle + c.c.$ (0.4766)
					$ H - 1 \rightarrow L + 1; H \rightarrow L + 1\rangle + c.c.$ (0.3324)
$3B_{3g}^-$	7.09	1.557	0.259		$ H \rightarrow L; H \rightarrow L + 1\rangle - c.c.$ (0.4407)
					$ H \rightarrow L + 2\rangle - c.c.$ (0.2124)
					$ H \rightarrow L + 2; H \rightarrow L + 3\rangle + c.c.$ (0.2044)
$4B_{3g}^-$	7.94	1.194	0.159		$ H \rightarrow L + 2; H \rightarrow L + 3\rangle + c.c.$ (0.2738)
					$ H \rightarrow L; H \rightarrow L + 4\rangle - c.c.$ (0.2424)
					$ H \rightarrow L; H \rightarrow L + 1\rangle + c.c.$ (0.2418)

Continued on next page

**Table V – continued from previous page**

State	E (eV)	Transition		Dipole (Å)	Wave Functions
		<i>x</i> -component	<i>y</i> -component		
					$ H \rightarrow L + 2\rangle + c.c.(0.2089)$
$5B_{3g}^-$	8.39	0.267	0.194		$ H - 4 \rightarrow L + 3\rangle + c.c.(0.3131)$
					$ H \rightarrow L + 3; H - 1 \rightarrow L + 3\rangle - c.c.(0.2058)$

## B. Anthracene

Table VI:  $A_g^-$ -type excited states contributing to the photo-induced absorption spectrum of anthracene, corresponding to transition from  $1B_{2u}^+$  (at 3.66 eV) and  $1B_{3u}^+$  state (at 5.34 eV) due to the absorption of  $y$ -polarized and  $x$ -polarized photons, respectively, computed using the FCI method coupled with the standard parameters in the PPP model Hamiltonian. The table includes many particle wave functions, excitation energies, and dipole matrix elements of various states with respect to  $1B_{2u}^+$  and  $1B_{3u}^+$  states. ‘+c.c.’ indicates that the coefficient of charge conjugate of a given configuration has the same sign, while ‘-c.c.’ implies that the two coefficients have opposite signs.

State	E (eV)	Transition	Dipole (Å)	Wave Functions
		$y$ -component	$x$ -component	
$2A_g^-$	3.89	0.150	-	$ H \rightarrow L; H \rightarrow L\rangle$ (0.5639)
				$ H \rightarrow L + 3\rangle + c.c.$ (0.3372)
				$ H - 1 \rightarrow L + 2\rangle + c.c.$ (0.2476)
$3A_g^-$	4.98	0.635	-	$ H \rightarrow L + 3\rangle - c.c.$ (0.3502)
				$ H \rightarrow L; H - 1 \rightarrow L + 1\rangle$ (0.3331)
				$ H \rightarrow L; H \rightarrow L\rangle$ (0.3015)
				$ H \rightarrow L; H - 2 \rightarrow L + 2\rangle$ (0.2562)
$4A_g^-$	5.14	0.434	-	$ H - 1 \rightarrow L + 2\rangle + c.c.$ (0.4913)
				$ H \rightarrow L; H \rightarrow L\rangle$ (0.3685)
				$ H \rightarrow L; H - 1 \rightarrow L + 1\rangle$ (0.2605)
$5A_g^-$	5.77	0.147	0.201	$ H \rightarrow L; H \rightarrow L + 4\rangle - c.c.$ (0.3709)
				$ H \rightarrow L + 6\rangle + c.c.$ (0.3412)
				$ H \rightarrow L; H - 2 \rightarrow L + 2\rangle$ (0.3095)
$6A_g^-$	6.45	0.304	0.233	$ H \rightarrow L; H - 2 \rightarrow L + 2\rangle$ (0.3396)
				$ H \rightarrow L + 2; H \rightarrow L + 2\rangle - c.c.$ (0.3212)
$7A_g^-$	7.16	-	0.627	$ H \rightarrow L; H - 1 \rightarrow L + 1\rangle$ (0.2204)
				$ H \rightarrow L + 1; H \rightarrow L + 1\rangle + c.c.$ (4153)
$8A_g^-$	7.30	0.155	0.691	$ H \rightarrow L; H - 1 \rightarrow L + 1\rangle$ (0.4150)
				$ H \rightarrow L; H - 1 \rightarrow L + 1\rangle$ (0.3325)
				$ H - 4 \rightarrow L + 3\rangle + c.c.$ (0.2810)
$10A_g^-$	7.92	0.348	0.403	$ H \rightarrow L + 2; H - 1 \rightarrow L + 3\rangle + c.c.$ (2137)
				$ H \rightarrow L; H - 4 \rightarrow L + 4\rangle$ (0.2027)
$10A_g^-$	7.92	0.348	0.403	$ H \rightarrow L; H - 1 \rightarrow L + 1\rangle$ (0.2848)
				$ H \rightarrow L; H - 2 \rightarrow L + 2\rangle$ (0.2178)



Table VII:  $B_{3g}^-$ -type excited states contributing to the photo-induced absorption spectrum of anthracene, corresponding to transition from  $1B_{2u}^+$  (at 3.66 eV) and  $1B_{3u}^+$  state (at 5.34 eV) due to the absorption of  $x$ -polarized and  $y$ -polarized photons, respectively, computed using the FCI method coupled with the standard parameters in the PPP model Hamiltonian. The table includes many particle wave functions, excitation energies, and dipole matrix elements of various states with respect to  $1B_{2u}^+$  and  $1B_{3u}^+$  states. ‘+c.c.’ indicates that the coefficient of charge conjugate of a given configuration has the same sign, while ‘-c.c.’ implies that the two coefficients have opposite signs.

State	E (eV)	Transition	Dipole (Å)	Wave Functions
		$x$ -component	$y$ -component	
$1B_{3g}^-$	4.31	1.037	-	$ H \rightarrow L + 2\rangle + c.c.(0.5226)$
				$ H \rightarrow L; H \rightarrow L + 1\rangle + c.c.(0.2808)$
$2B_{3g}^-$	6.37	-	0.278	$ H \rightarrow L + 2\rangle - c.c.(0.6268)$
$3B_{3g}^-$	6.68	1.168	0.126	$ H - 1 \rightarrow L + 3\rangle - c.c.(0.3000)$
				$ H \rightarrow L; H \rightarrow L + 1\rangle + c.c.(0.2970)$
$4B_{3g}^-$	6.98	-	0.155	$ H - 4 \rightarrow L + 2\rangle + c.c.(0.3138)$
				$ H \rightarrow L + 1; H \rightarrow L + 4\rangle + c.c.(0.2492)$
$5B_{3g}^-$	7.39	1.253	0.245	$ H - 2 \rightarrow L + 2; H \rightarrow L + 1\rangle + c.c.(0.2496)$
				$ H \rightarrow L; H \rightarrow L + 1\rangle - c.c.(0.2449)$
				$ H \rightarrow L; H - 1 \rightarrow L + 4\rangle + c.c.(0.2101)$
				$ H - 4 \rightarrow L + 2\rangle + c.c.(0.2009)$
$6B_{3g}^-$	7.77	1.313	0.329	$ H \rightarrow L; H \rightarrow L + 1\rangle - c.c.(0.2409)$
				$ H \rightarrow L + 2; H \rightarrow L + 3\rangle + c.c.(0.2293)$

Table VIII:  $A_g^-$ -type excited states contributing to the photo-induced absorption spectrum of anthracene, corresponding to transition from  $1B_{2u}^+$  (at 3.55 eV) and  $1B_{3u}^+$  state (at 4.64 eV) due to the absorption of  $y$ -polarized and  $x$ -polarized photons, respectively, computed using the FCI method coupled with the screened parameters in the PPP model Hamiltonian. The table includes many particle wave functions, excitation energies, and dipole matrix elements of various states with respect to  $1B_{2u}^+$  and  $1B_{3u}^+$  states. ‘+c.c.’ indicates that the coefficient of charge conjugate of a given configuration has the same sign, while ‘-c.c.’ implies that the two coefficients have opposite signs.

State	E (eV)	Transition	Dipole (Å)	Wave Functions
		$y$ -component	$x$ -component	
Continued on next page				

Table VIII – continued from previous page

State	E (eV)	Transition		Wave Functions
		<i>y</i> -component	<i>x</i> -component	
$3A_g^-$	4.27	0.782	-	$ H \rightarrow L + 3\rangle + c.c.(0.3743)$
				$ H \rightarrow L; H - 1 \rightarrow L + 1\rangle (0.3083)$
				$ H \rightarrow L; H \rightarrow L\rangle (0.2538)$
				$ H \rightarrow L; H - 2 \rightarrow L + 2\rangle (0.2284)$
$4A_g^-$	4.62	0.461	-	$ H \rightarrow L + 3\rangle + c.c.(0.4822)$
				$ H \rightarrow L; H \rightarrow L\rangle (0.3492)$
				$ H \rightarrow L; H - 1 \rightarrow L + 1\rangle (0.2122)$
$5A_g^-$	5.28	0.139	-	$ H \rightarrow L; H \rightarrow L + 4\rangle - c.c.(0.3492)$
				$ H \rightarrow L + 6\rangle - c.c.(0.3427)$
				$ H \rightarrow L; H - 2 \rightarrow L + 2\rangle (0.2860)$
$6A_g^-$	5.72	0.536	0.453	$ H \rightarrow L; H - 2 \rightarrow L + 2\rangle (0.3011)$
				$ H \rightarrow L + 2; H \rightarrow L + 2\rangle + c.c.(0.2867)$
$7A_g^-$	6.45	0.178	1.767	$ H \rightarrow L; H - 1 \rightarrow L + 1\rangle (0.5117)$
				$ H - 3 \rightarrow L + 4\rangle - c.c.(0.2266)$
				$ H \rightarrow L + 1; H \rightarrow L + 1\rangle + c.c.(0.2084)$
$9A_g^-$	6.62	-	1.038	$ H - 4 \rightarrow L + 3\rangle + c.c.(0.2661)$
				$ H \rightarrow L; H - 1 \rightarrow L + 1\rangle (0.2513)$
$10A_g^-$	7.11	0.373	0.403	$ H \rightarrow L; H - 2 \rightarrow L + 2\rangle (0.2783)$
				$ H \rightarrow L; H - 1 \rightarrow L + 1\rangle (0.2491)$
				$ H - 2 \rightarrow L + 2; H \rightarrow L + 4\rangle + c.c.(0.2076)$
$11A_g^-$	7.34	0.834	1.437	$ H \rightarrow L + 3\rangle + c.c.(0.2264)$
				$ H - 2 \rightarrow L + 5\rangle + c.c.(0.2144)$
				$ H \rightarrow L; H - 1 \rightarrow L + 1\rangle (0.2128)$
				$ H \rightarrow L; H \rightarrow L\rangle (0.2086)$
$12A_g^-$	7.63	0.206	-	$ H \rightarrow L + 1; H - 3 \rightarrow L + 2\rangle + c.c.(0.2416)$
				$ H - 1 \rightarrow L + 1; H - 2 \rightarrow L + 2\rangle (0.2401)$

Table IX:  $B_{3g}^-$ -type excited states contributing to the photo-induced absorption spectrum of anthracene, corresponding to transition from  $1B_{2u}^+$  (at 3.55 eV) and  $1B_{3u}^+$  (at 4.64 eV) states due to the absorption of  $x$ -polarized and  $y$ -polarized photons, respectively, computed using the FCI method coupled with the screened parameters in the PPP model Hamiltonian. The table includes many particle wave functions, excitation energies, and dipole matrix elements of various states with respect to  $1B_{2u}^+$  and  $1B_{3u}^+$  states. ‘+c.c.’ indicates that the coefficient of charge conjugate of a given configuration has the same sign, while ‘-c.c.’ implies that the two coefficients have opposite signs.

State	E (eV)	Transition		Wave Functions
		$x$ -component	$y$ -component	
$1B_{3g}^-$	3.86	1.593	-	$ H \rightarrow L + 2\rangle + c.c.(0.5375)$ $ H \rightarrow L; H \rightarrow L + 1\rangle - c.c.(0.2162)$
$2B_{3g}^-$	5.52	0.971	0.373	$ H - 1 \rightarrow L + 3\rangle + c.c.(0.3189)$ $ H - 1 \rightarrow L + 1; H \rightarrow L + 1\rangle + c.c.(0.2503)$ $ H \rightarrow L; H \rightarrow L + 1\rangle - c.c.(0.2053)$
$3B_{3g}^-$	5.81	1.612	0.140	$ H \rightarrow L; H \rightarrow L + 1\rangle - c.c.(0.3673)$ $ H - 1 \rightarrow L + 3\rangle + c.c.(0.3316)$
$4B_{3g}^-$	6.21	0.613	0.153	$ H - 4 \rightarrow L + 2\rangle + c.c.(0.4228)$
$5B_{3g}^-$	6.43	1.271	0.174	$ H \rightarrow L; H \rightarrow L + 5\rangle + c.c.(0.2224)$ $ H - 2 \rightarrow L + 2; H \rightarrow L + 1\rangle + c.c.(0.2040)$
$6B_{3g}^-$	6.75	1.050	0.220	$ H \rightarrow L + 2; H \rightarrow L + 3\rangle + c.c.(0.2451)$